Open Access **Baghdad Science Journal** **P-ISSN: 2078-8665**
Published Online First: April, 2023 **2023, 20(6): 2224-2233** **E-ISSN: 2411-7986**

DOI: https://dx.doi.org/10.21123/bsj.2023.7637

Corrosion Inhibition Efficiency Investigation of Yttrium Oxide Nanoparticles Coated on Carbon Steel Alloy

Maha J. Hassin ***Taghried A. Salman****

Department of Chemistry, College of Science, Al-Nahrain University, Baghdad, Iraq
*Corresponding author: dr.tag_s@yahoo.com
E-mail address: mahaaltemmemy1951@gmail.com.

Received 2/9/2022, Revised 2/12/2022, Accepted 4/12/2022, Published Online First 20/4/2023, Published 01/12/2023

Abstract:

Metal oxide nanoparticles demonstrate uniqueness in various technical applications due to their suitable physiochemical properties. In particular, yttrium oxide nanoparticle(Y_2O_3NPs) is familiar for technical applications because of its higher dielectric constant and thermal stability. It is widely used as a host material for a variety of rare-earth dopants, biological imaging, and photodynamic therapies. In this investigation, yttrium oxide nanoparticles (Y_2O_3NPs) was used as an ecofriendly corrosion inhibitor through the use of scanning electron microscopy (SEM), Fourier transforms infrared spectroscopy (FT-IR), UV-Visible spectroscopy, X-ray diffraction (XRD), and energy dispersive X-ray spectroscopy(EDX), the physico-chemical characterization of Y_2O_3NPs was examined. The primary characteristic peak of YOY at 565 cm^{-1}, which indicates the synthesis of nanoparticles, is seen in the FT-IR spectra. The XRD pattern showed that a single phase cubic structure of YONPs with an Ia-3 space group had formed. SEM was used to examine the surface morphology. The composition of Yttrium and oxygen in Y_2O_3NPs was determined to be 78.74% and 21.26%, respectively, according to the EDX results. The anticorrosive behavior was tested by polarization curve in 18.204% $CaCl_2$ solution at five temperatures in the range 293- 313 K. Various concentrations 0.15 0.26 and 0.37 of N Y_2O_3NPs coating on the carbon steel surface were applied using the electrophoresis deposition method. The obtained results indicated that Y_2O_3NPs formed a protective film acts as a physical barrier for the protection of steel alloy. Additionally, corrosion protection efficiency values of 0.26 N Y_2O_3NPs coating were superior to that of 0.15 and 0.37 N Y_2O_3NPs coating, respectively.

Keywords: Anticorrosion investigation, Carbon steel, Electrophoresis deposition, Polarization, Yttrium oxide nanoparticles.

Introduction:

The majority of economies in the world rely heavily on the transportation and distribution of resources, including oil, gas, chemicals, water, steam, and petroleum products. They play a significant role in our infrastructure. Electrochemical degradation, sometimes known as corrosion, poses a serious danger to the integrity of these important assets[1]. An electrochemical reaction in an aqueous medium, often soil water or portions of the goods they carry, results in the corrosion of pipelines. The process of electron transfer is a crucial part of corrosion. Most corrosion integrity management solutions include monitoring and mitigation systems that keep an eye on the voltages and currents connected to the corrosion process[2,3]. Recent studies have shown that nano coating materials are essential for increasing corrosion resistance in challenging environments, improving mechanical qualities, and minimizing dimension changes. In addition to corrosion resistance, mechanical characteristics, making it smoother, stronger, and improving its adhesive qualities are just a few of the numerous advantages that may be realized thanks to nano coating's exceptional capabilities[4]. One kind of valuable rare earth element called yttrium oxide (Y_2O_3), an inorganic nanoparticle, has appealing antibacterial and antioxidant properties[5]. Numerous studies claim that Y_2O_3 has greater levels of hardness and is chemically stable[6–8]. The corrosion resistance and toxicity of yttrium oxide are both high[9]. Recapitulated are the chemical processes used to create nanoparticles, including sol-gel, emulsion,

solid-state reactions, combustion, colloid reaction techniques, and hydrothermal processing[5]. However, these procedures are expensive, harmful to the environment, and fraught with biological dangers[10]. Due to the availability of several natural resources, inexpensive, and non-toxic ingredients, the production of nanoparticles from plant extracts has considerably increased[11]. Renal carcinoma cells have been effectively inhibited by greenly produced Y_2O_3NPs. The synthesis process is an affordable, environmentally sustainable, and alternative to physical and chemical procedures with less negative side effects[12]. Green synthesis of yttrium oxide (Y_2O_3) nanoparticles using lantana camara leaf extracts have been studied[13].

These nanoparticles were characterized with the aid of different methods, including UV, X-ray diffraction (XRD), Fourier transformed infrared spectroscopy (FTIR), transmitted electron microscopy (TEM), and photocatalytic degradation. Y2O3 nanoparticles showed an excellent antibacterial activity against Gram-positive Bacillus subtilis and Gram-negative *Escherichia coli* with a 10 to 15 mm inhibitory zone. Green Y_2O_3NPs were released with a 4 hours lag time and 80% sustained release rate, indicating that they could be used in drug delivery. In addition, the bioavailability of green Y2O3 NPs was investigated using cell viability in cervical cancer cell lines. A low-cost electrochemical method called electrophoretic deposition (EPD) that can be used at room temperature and deposit several components simultaneously in a single coating phase has made it possible to create multifunctional coatings[14–17]. In addition, EPD may be used to coat complex-shaped samples since it can be applied to any solid in the form of powders that can be dispersed in a solvent to create stable suspensions[18,19]. The fabrication of micro- and nanostructured ceramics using this method is possible for a variety of uses, including biological, optical, and corrosion protection[20].

In the present study, yttrium oxide nanoparticles were used. The structure, morphology and formation of YONPs were characterized by various techniques including FT-IR, UV-Visible, XRD and SEM-EDX analysis. The electrochemical studies were carried out in $CaCl_2$ solution using various temperatures and concentrations of YONPs coating on mild steel surface through electrophoresis deposition technique. kinetic and thermodynamic parameters of the coated and uncoated sample were also measured.

Materials and Methods:

1. Materials

Carbon steel alloy was used to build the water application pipes in Iraq. The carbon steel used in this research has the following weight percentage composition: P (0.018), Mo (0.03), Ni (0.017), C (0.19), Si (0.35), Cr (0.04), Cu (0.02), Al (0.06), and the rest was iron as revealed by emission spectroscopic analysis. Chemicals of analytical reagent grade were used to prepare the solutions. Working electrodes were formed in the shape of cylindrical objects and had a surface area of 1 cm^2. The sample was polished to a mirror finish using emery paper of various grades 320, 500, 1000, 2400, and 4000, a diamond product spray, aqueous ethanol and diamond particles of various sizes 1, 3, 6, and 9 mm, and lastly, distilled water as a final rinse.

2. Solutions Preparation

Dissolving 182.04 g of $CaCl_2$ in 1000 mL of distilled water yielded an 18.204% calcium chloride solution. Yttrium oxide nanoparticles (Sigma-Aldrich) (99.9% purity) coating solution, in various concentrations 0.15, 0.26, 0.37 N, was prepared by dissolving 0.3, 0.5, and 0.7 grams of Y_2O_3NPs in 50 ml of acetyl acetone, adding a small amount of iodine to the solution to increase its conductivity.

3. Electrophoresis Deposition

The yttrium oxide nanoparticles were electrophoretically deposited (EPD) onto a carbon steel substrate utilizing a direct current (DC) power supply with a voltage range of 0 to 15 V. The circuit is employed by the AC meter to measure the current created between the electrodes, and a 50 ml covered beaker contains two slits with a distance of 1 cm between them. Meanwhile, a stainless steel tong is used to catch the carbon steel specimen as well as the carbon steel rod that serves as the inert electrode in the deposition process cell. The deposition of specimens takes place over a period of 5 to 30 minutes, after which the sample is left at room temperature for 24 hours to dry gradually. A thick film was applied to carbon steel surface after the EPD technique described above to ensure a homogeneous coating.

4. Electrochemical Studies

To perform electrochemical measurement, this is done by using electrochemical System Potentiostat/Galvanostat (M Lab (WENKING MLab multichannel and SCI-MLab system for corrosion measurement obtained from Bank Electronics-Intelligent controls GmbH, Germany 2007) , the M-Lab works on a desktop computer (Windows XP). To

perform corrosion measurements, the device is attached to a corrosion cell made up of three electrodes: a carbon steel alloy for the working electrode, a platinum electrode for auxiliary purposes, and a saturated Calomel electrode (SCE) for reference purposes. Eq. 1, is used to calculate the percentage of inhibition efficiency (%IE) of yttrium oxide against corrosion of a carbon steel sample in calcium chloride solution [21].

$$IE\ (\%) = [\ (\ i^{o}_{corr} - i_{corr}) / i^{o}_{corr}] \times 100 \quad \ldots..1$$

Where , i^{o}_{corr} corrosion current density for blank and i_{corr} corrosion current density of a carbon steel coated with different concentrations of nano- yttrium oxide at the same temperature.

The surface coverage (θ) of carbon steel by (Y_2O_3)NP is estimated by using Eq. 2[21]:

$$\theta = (\%\ IE/\ 100) \quad \ldots\ldots 2$$

Results and Discussion:

1. Polarization Measurements

The polarization curves for corrosion of carbon steel in 18.204 % $CaCl_2$ solution for blank and various concentrations of Y_2O_3 NP coatings at different temperatures 293, 298,303,308 and 313 K are illustrated in Fig.1 (a, b, c and d). Electrochemical parameters as corrosion current density (i_{corr}), corrosion potential(E_{corr}), cathodic (bc), and anodic (ba) Tafel slopes are given in Table. 1.

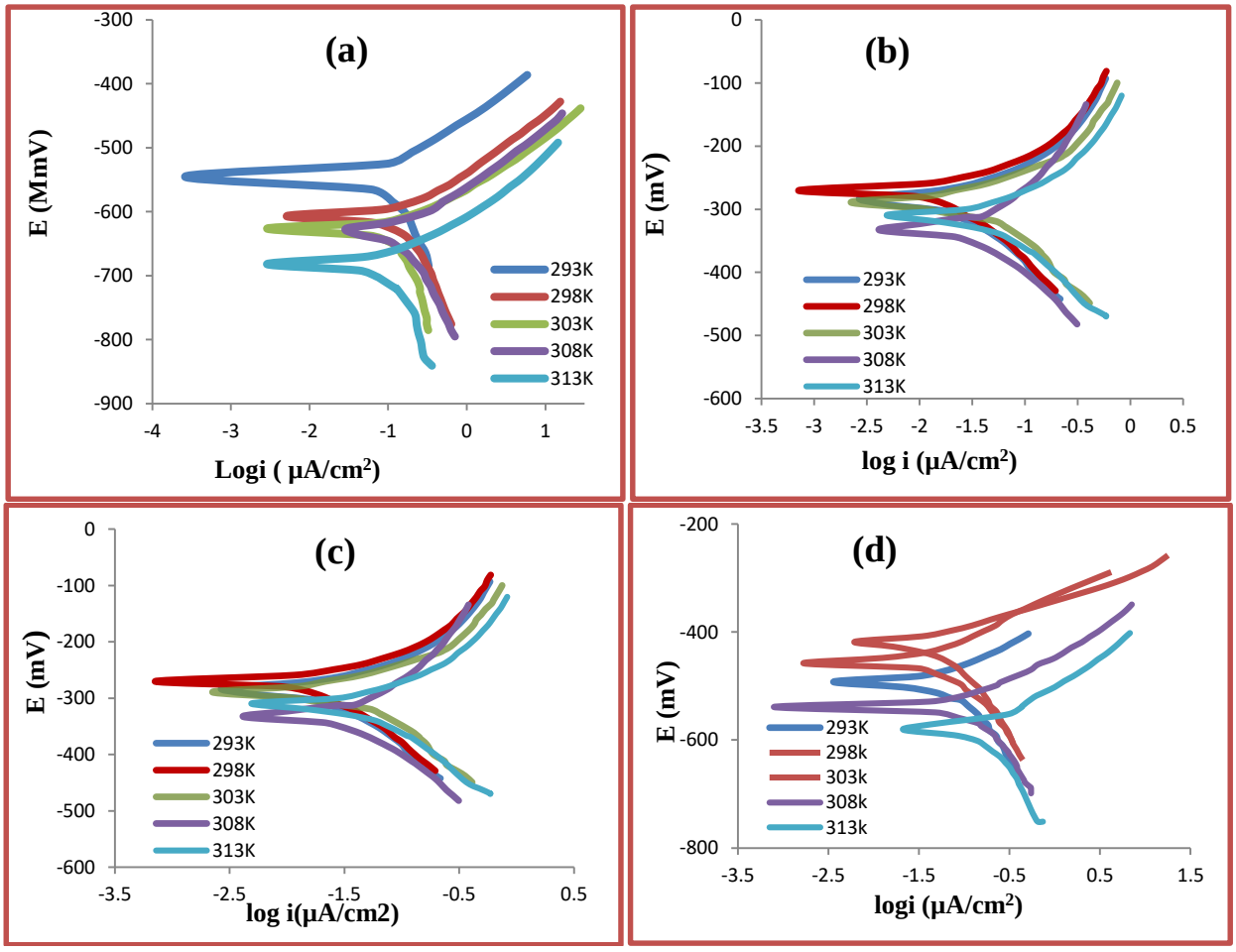

Figure 1. Polarization curves for carbon steel corrosion in (18.204 %) $CaCl_2$, a-blank, b- 0.15 N , c-0.26 N ,d-0.37N coated with Y_2O_3NP concentrations at a temperature range (293-313) K.

Table 1. Corrosion parameters of carbon steel in (18.204 %) $CaCl_2$ for uncoated and coated alloy with different Y_2O_3 NPs concentrations 0.15, 0.26 and 0.37 N at a temperature range (293-313)K.

Inh(N)	T(K)	$-E_{corr}$ (MV)	i_{corr} ($\mu A/cm^2$)	Tafel slop (mV/dec)		θ	%IE
				-bc	+ba		
-	293	600	68.24	185.8	75.8	-	-
	298	605	123.2	181.3	72.9	-	-
	303	626	146.9	245.8	77.7	-	-
	308	632	156.9	143.9	71.1	-	-
	313	693	162.1	135.5	68.4	-	-
0.15	293	336	10.35	109.9	91.0	0.84832	84.8329
	298	337	11.12	137.4	128.9	0.90974	90.9740
	303	337	12.72	95.0	69.5	0.91341	91.3410
	308	354	15.14	103.3	70.4	0.90350	90.3500
	313	374	20.75	122	89.7	0.87199	87.1990
0.26	293	269	10.2	85	51.2	0.85052	85.0528
	298	281	11.11	76.3	43.9	0.90982	90.9821
	303	290	12.5	95.1	50	0.91491	91.4908
	308	332	13.11	109.4	104.3	0.92098	92.0976
	313	338	17.54	106.3	75.4	0.89179	89.1795
0.37	293	410	19.06	100.2	46.6	0.72069	72.0692
	298	419	22.66	94.4	51.5	0.81607	81.6070
	303	458	31.14	90.1	84.6	0.78801	78.8010
	308	538	51.89	83.3	65.6	0.67495	67.4950
	313	580	68.38	84.3	53.9	0.57816	57.8160

The data obtained listed in Table. 1, indicates the following :-

1- Coating the carbon steel alloy with yttrium oxide nanoparticles and with concentration mentioned in Table 1 indicates the diffraction of the voltage in the direction of an increase in negative values from the equilibrium potential, which means that the protection we obtained is cathodic protection[22].

2- It has been observed that the rate of corrosion increased with increasing the temperature because temperature accelerates corrosion process such as electrochemical reaction, chemical reaction, and the process of transferring of reactive species to the metal surface[23].

3- At the concentrations of 0.15 and 0.26 N, it was found that increasing the concentration with growing temperature increases the efficiency of inhibition, as it was noticed that the activation energy increase (Table 2) from 30.25 kJ/ mol at 0.15N to 51.55 kJ/ mol at 0.26, which is an evidence of the occurrence of chemical adsorption between the Y_2O_3NPs and the metal surface[24].

4- At the concentration 0.37N, an increase in the corrosion rate and decrease in the inhibition efficiency was observed due to occurrence of agglomeration in the Y_2O_3 NPs deposited on the metal surface[24]. Activation energy data (Table 2) increases with increasing concentration which is an evidence of the occurrence of physical adsorption that is the bonding of Y_2O_3NPs through Van der Waals forces with the metal surface[25].

2. Thermodynamics Parameters

Thermodynamic parameters of the corrosion reaction includes activation energy Ea ,entopy ΔS* and enthalpy ΔH* of activation were calculated using Arrhenius Eq. 3[26] :-

$$\text{Log CR} = \log A - \frac{Ea}{2.303\ RT} \quad \text{.....3}$$

While the transition state equation is calculated from the Eq. 4 below[26].

$$\text{Log}\frac{CR}{T} = \log\left(\frac{R}{Nh}\right) + \frac{\Delta S^*}{2.303R} - \frac{\Delta H^*}{2.303RT} \quad \text{.....4}$$

Where

CR: corrosion rate, Ea: the apparent activation energy, R: universal gas constant 8.314 J mol^{-1} K^{-1}, T : temperature, A: the Arrhenius pre-exponential factor, h : Plank's constant 6.626176 x 10^{-34} J.s., N : Avogadro's number 6.022 x 10^{23} mol^{-1}, ΔS^* is the entropy of activation and ΔH^* is the enthalpy of activation. The log corrosion rate is plotted against 1/T for the blank and Y_2O_3NPs coated carbon steel in $CaCl_2$ solution as shown in Fig.2. The log CR/T is plotted against 1/T for the blank and Y_2O_3NPs coated carbon steel in $CaCl_2$ solution and ΔH^*, ΔS^* values were obtained, respectively from the slop and intercept as presented in Fig.3. Data obtained is tabulated in Table. 2.

Baghdad Science Journal
2023, 20(6): 2224-2233
P-ISSN: 2078-8665
E-ISSN: 2411-7986

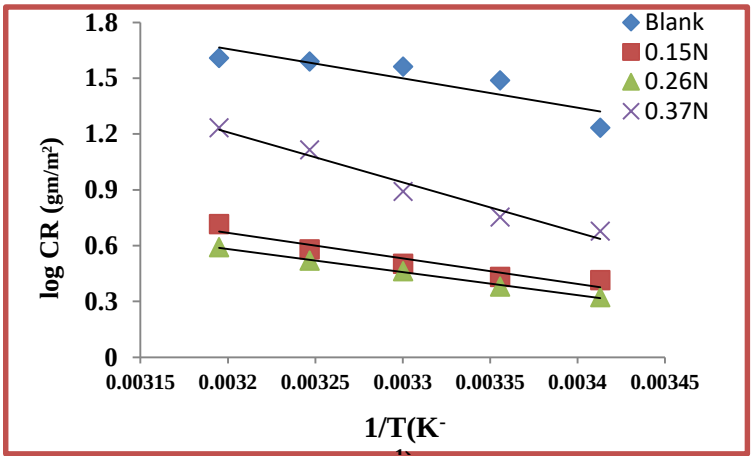

Figure 2. Plot of log CR against 1/T of carbon steel in 18.204 % $CaCl_2$ solution for uncoated and coated carbon steel with different Y_2O_3NPs concentrations.

Table 2. Thermodynamic values of the coated and un coated carbon steel in 18.204 % $CaCl_2$ at different concentration of Y_2O_3 NPs and temperatures.

CS	Ea(kJ/mol)	A(molecule $cm^{-2}.s^{-1}$)	ΔH* (kJ/mol)	ΔS* (J/mol .K)	ΔG* (kJ/mol)
Blank	30.25	3.098×10^{30}	27.725	-124.89	64.317
					64.942
					65.566
					66.191
					66.815
0.15	46.23	6.7945×10^{28}	23.7118	-156.67	69.617
					70.401
					71.184
					71.967
					72.751
	63.73	2.127×10^{28}	21.215	-166.328	69.949
0.26					70.781
					71.613
					72.444
					73.276
0.37	51.55	4.022×10^{33}	49.035	-65.280	68.164
					68.491
					68.817
					69.144
					69.470

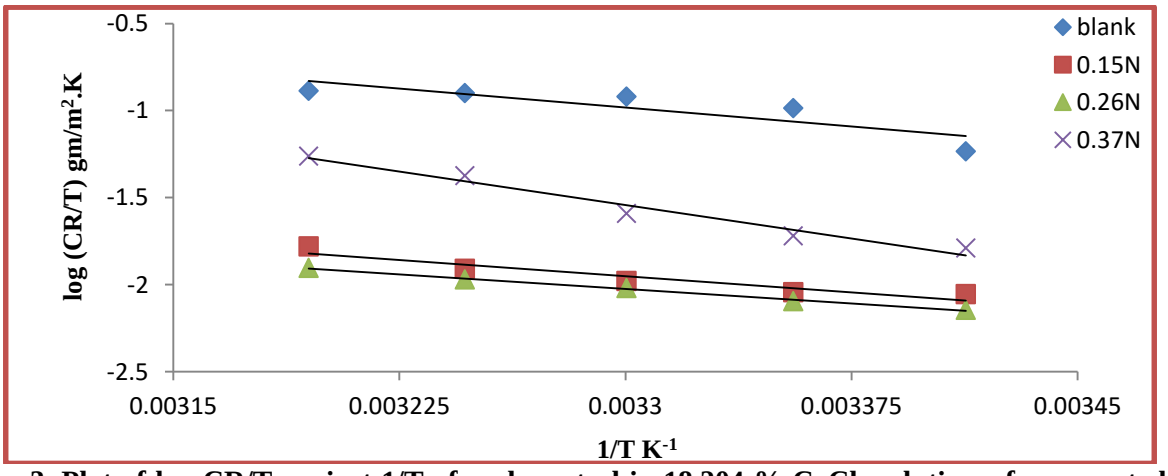

Figure 3. Plot of log CR/T against 1/T of carbon steel in 18.204 % $CaCl_2$ solution for uncoated and coated carbon steel with different Y_2O_3NPs concentrations.

From Fig. 2, it is observed that the relationship between corrosion rate and temperature is linear , and the corrosion rate decrease when the concentration of the inhibitor is 0.15N and 0.26N , but the corrosion rate increased at 0.37N to be close to the corrosion rate of blank , as mentioned previously due to agglomeration in yttrium oxide nanoparticles, the nature of the bonding of molecules to the metal surface is physical adsorption[23,27]. The negative values of ΔS* reveal that the activated complex in the rate determining step represents association rather than the dissociation step, this means a decrease in disorder take place[28].

4.Characterization

The Y_2O_3 nanoparticles were characterized by UV-Visible, FTIR, XRD, SEM, and AFM techniques.

Y_2O_3 nanoparticles were optically measured using a UV-visible absorbance spectrophotometer. The UV–visible spectrum of the examined nanoparticles was recorded in the range (200–800 nm) using a Varian, Cary 5000 with a scanning rate of (600nm/min). Y_2O_3 nanoparticles were optically measured using a UV-visible absorbance spectrophotometer at room temperature. The advent of Y_2O_3's yttrium adsorption in the UV band at 284.0 nanometres is a sign of the nano scale[28]. The absorption spectrum of nano yttrium oxide is shown in Fig.4.

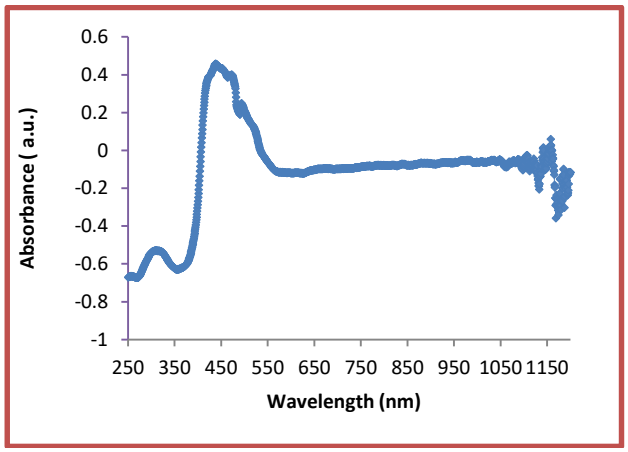

Figure 4. UV-Visible spectrum of Y_2O_3 nanoparticles.

FT-IR spectroscopy was used to analyse yttrium oxide nanoparticles; the spectrum was recorded in the range 400-4000 cm^{-1}. The FT-IR spectrum of Y_2O_3 is shown in Fig.5 where a sharp peak that appeared at 565 cm^{-1} is an evidence of absorption Y-O stretching vibration, the peak at 588 cm^{-1} corresponds to the anti-symmetric Y–O–Y stretching. The peak at 873 cm^{-1} is responsible for the presence of trace of Y–OH. The peaks at 1216, 1085 and 1026 cm^{-1} are the characteristic asymmetric stretching of Y–O–Y present in the nanostructure[29]. The appearance of the result in Fig. 5 is closed to[29] above where we find the appearance of its absorption by functional groups: At 560.61 cm^{-1} : Y-O (sharp peak) stretching vibration 676.02 cm^{-1} : O-Y-O anti symmetric stretching 848.49 cm^{-1}:Y-OH trace amount 1510.9-1404.3 cm^{-1} asymmetric stretching.

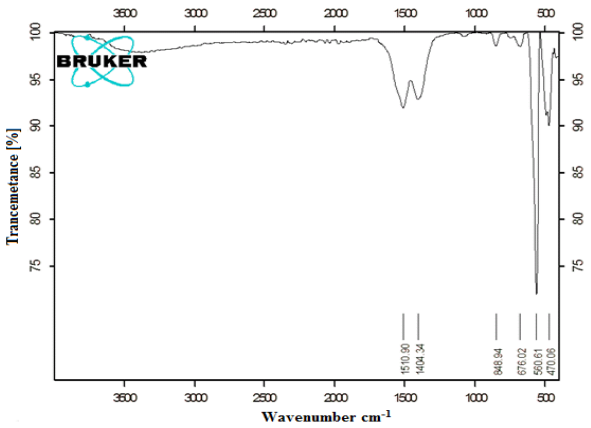

Figure 5. FT-IR spectrum of Y_2O_3 nanoparticles.

To further investigate the structural properties of nano –Y_2O_3, we used XRD technique. Fig. 6 shows the XRD pattern of Y_2O_3 nanoparticles. The result obtained from XRD indicated that the Y_2O_3 has single phase cubic structure with Ia-3 space group. In addition, there were no any peaks in any phase or impurities in the XRD graph .

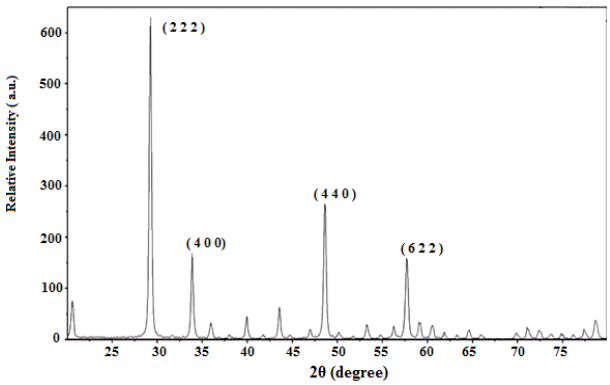

Figure 6. XRD pattern of Y_2O_3 nanoparticles.

SEM – (SIGMA HV – Carl Zeiss with Bruker Quantax 200 – Z10 EDS Detector) were used to measure the surface morphology (The shape and size of the particles). Fig. 7 shows SEM image of pure Y_2O_3 nanoparticles. It was noticed that the surface of the Y_2O_3 NPs is uniform and homogeneous with the observation of a little agglomeration of nanoparticles, but it takes a regular geometric shapes.

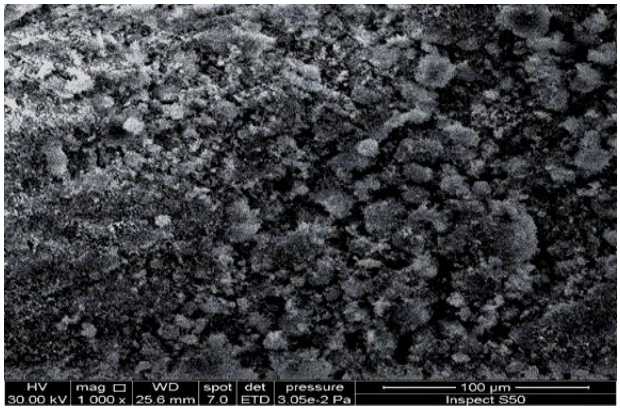

Figure 7. SEM image of Y_2O_3 nanoparticles.

To determine the chemical composition of nanoparticles, an EDX analysis was obtained. Fig. 8 shows the EDX spectrum of Y_2O_3 NPs, where only Y and O are shown; this indicates that the material is pure and does not contain impurities.

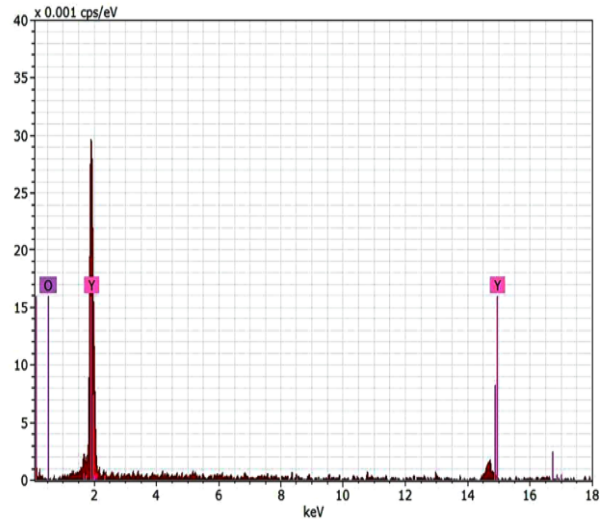

Figure 8. EDX spectrum of Y_2O_3 nanoparticles.

AFM is an effective method for statically assessing the distribution of particle sizes as well as investigating surface shape at the nano to micro scale. Fig. 9 shows an AFM image of pure yttrium oxide nanoparticles where the particle diameter, surface roughness, surface waves and three dimensional shape are shown. The lower the roughness values, the more corrosion resistance[30]. In the AFM result below, the surface roughness is very low which is evidence that the nanomaterials have a high corrosion resistance. We note from the result that agglomeration of particle occurs and the highest agglomeration occurs at 45 nm diameter for the agglomerated particles.

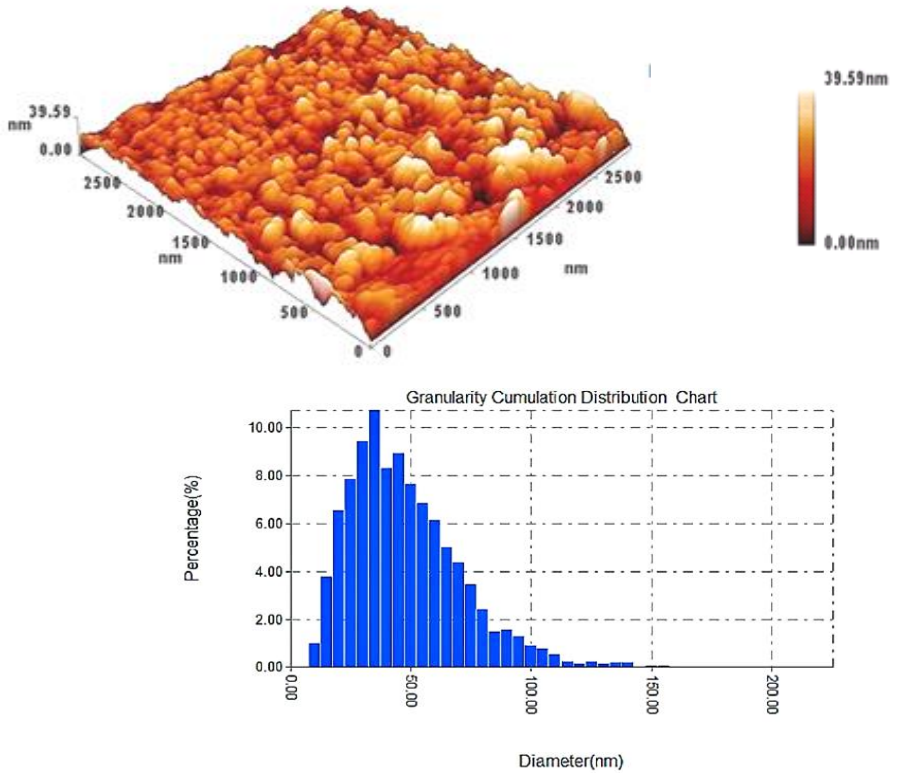

Figure 9. AFM images of Y_2O_3 nanoparticles.

Conclusions:

Y_2O_3NPs were successfully deposited on a carbon steel alloy surface by using an electrophoretic deposition technique. The layer deposited of these nanoparticles on the metal surface was characterized using various techniques, such as UV-visible, FT-IR, X-ray diffraction, SEM, and AFM. XRD data revealed that Y_2O_3NPs were pure single-phase cubic structures. The AFM result indicates that the surface roughness is very low, which is evidence that the nanomaterials have high corrosion resistance. We note from the result that agglomeration of particles occurs and the highest agglomeration occurs at 45 nm in diameter for the agglomerated particles. SEM image of pure Y_2O_3 nanoparticles indicates that the surface of the Y_2O_3 NPs is uniform and homogeneous with the observation of a little agglomeration of nanoparticles, but it takes a regular geometric shape. The percentage of corrosion inhibition of Y_2O_3NPs was found to be high, especially at a nanoparticle concentration of 0.26 N as observed from corrosion rate data, which is lower than the other concentrations. Additionally, increasing the temperature decreases the inhibition efficiency at all concentrations and it was found that increasing the concentration of the inhibitor above 0.26 N increases the corrosion rate due to the agglomeration of the nanomaterial on the alloy surface. Thermodynamic studies reveal that the nature of the bonding of molecules to the metal surface is physical adsorption. The negative values of ΔS* reveal that the activated complex in the rate determining step represents association rather than dissociation. This means a decrease in disorder takes place.

Authors' Declaration:

- Conflicts of Interest: None.
- We hereby confirm that all the Figures and Tables in the manuscript are mine ours. Besides, the Figures and images, which are not mine ours, have been given the permission for re-publication attached with the manuscript.
- Ethical Clearance: The project was approved by the local ethical committee in Al-Nahrain University.

Authors' Contributions Statement:

M. J. H. performed the measurements, planning, and processed the experimental data. T. A. S. performed the analysis, drafted the manuscript, designed the figures, assisted in interpreting the results, and worked on the manuscript. Both authors discussed the results and commented on the manuscript.

References:

1. Mohammed KA. Corrosion control mechanisms and the effect of pH on corrosion in the crude oil refining process. J Pet Sci Res. 2022; 34 (2): 270-289. https://doi.org/10.52716/jprs.v12i1(Suppl.).637
2. Kantor M M, Sudin V V, Solntsev KA. Materials science aspects of stress corrosion cracking of Russian pipelines. E3S Web Conf. 2019; 121, 04014. https://doi.org/10.1051/e3sconf/201912104014
3. Jones DA. Principles and prevention of corrosion, 2nd ed , New Jersey: Prentice Hall. 1996;474.
4. Al-Juboori SA, Al-shamaileh D. Improving the corrosion resistance of carbon steel cylindrical pipe by Nano- materials Coating. Part-1. Int Sci J. 2021; 3 : 110-116. https://doi.org/10.30684/etj.v39i6.2009
5. Rajakumar G, Mao L, Bao T, Wen W, Wang S, Gomathi NG, Rebezov M, Shariati MA, Chung I, Thiruvengadam M, Zhang X. Yttrium oxide Nanoparticle Synthesis: An Overview of Methods of preparation and Biomedical Applications. Appl Sic. 2021; 11:2172-2180. https://doi.org/10.3390/app11052172
6. Rastogi AC, Sharma RN. Interfacial charge trapping in extrinsic Y_2O_3/SiO_2 bilayer gate dielectric based MIS devices on Si(100). Semicond Sci Technol. 2019; 16:641–650.https://doi.org/10.1088/0268-1242/16/8/301
7. Wu CH, Chen JZ. Ultrafast atmospheric-pressure-plasma-jet processed conductive plasma-resistant Y_2O_3/carbon-nanotube Nanocomposite. J Alloy Compd. 2018; 651:357–362. https://doi.org/10.1016/j.jallcom.2015.08.085
8. Xu YN, Gu ZQ, Ching WY. Electronic, structural, and optical properties of crystalline yttrium. Phys Rev B. 1997; 56: 14993–15000. https://doi.org/10.1103/PhysRevB.56.14993
9. Du P, Luo L, Yue Q, Li W. The simultaneous realization of high and low temperature thermometry in Er^{+3} / Yb^{+3} codoped Y_2O_3 nanoparticles. Mater Lett.2018; 143(15): 209-211. https://doi.org/10.1016/j.matlet.2018.12.123
10. Arsiya F, Sayadi MH, Sobhani S. Green synthesis of palladium nanoparticles using Chlorella vulgaris. Mater Lett. 2016; 186: 113–115. https://doi.org/10.1016/j.matlet.2016.09.101
11. Khamhaengpola A, Sirib S. Green synthesis of silver nanoparticles using tissue extract of weaver ant larvae. Mater.Lett. 2017; 192: 72–75. http://dx.doi.org/10.1016/j.matlet.2017.01.076
12. Nagajyothi PC, Pandurangan M, Veerappan M, Kim DH, Sreekanth TM, Shim J. Green synthesis, characterization and anticancer activity of yttrium oxide nanoparticles. Mater Lett. 2017; 12: 81-90.https://doi.org/10.1016/J.MATLET.2017.12.081
13. Rajakumar G, Mydhili G, Salman S, Preeyanghaa , Neppolian , Thandapani , Mohammad A, Mohammad N, Banan A, Shaheer M, Devi R, Kaliaperumal R, Saleh A, Muthu Th. Sustainable green synthesis of yttrium oxide (Y_2O_3) nanoparticles using lantana camara leaf extracts: physicochemical characterization, photocatalytic degradation, antibacterial, and anticancer potency. Nanomaterials.

2022; 12: 2393-2407. https://doi.org/10.3390/nano12142393
14. Rojaee R, Fathi M, Raeissi K, Taherian M. Electrophoretic deposition of bioactive glass nanopowder on magnesium based alloy for biomedical applications. Ceram Int. 2013; 40: 7879–7888. https://doi.org//10.1016/j.ceramint.2013.12.135
15. Boccaccini AR, Keim S, Li Y, Zhitomirsky I. Electrophoretic deposition of biomaterials. J R Soc Interface. 2017; 7 (5):581–613. https://doi.org/10.1098/rsif.2010.0156.focus
16. Chávez-Valdez A, Boccaccini AR. Innovations in electrophoretic deposition:Alternating current and pulsed direct current methods. Electrochim Acta. 2012; 65: 70–89. https://doi.org/10.1016/j.electacta.2012.01.015
17. Heise S. Electrophoretic deposition of gelatine nanoparticle/chitosan coatings. Electrochimica Acta. 2019; 307 :318-325. https://doi.org/10.1016/j.electacta.2019.03.145
18. Van der Biest OO, Vandeperre LJ. Electrophoretic Deposition of Materials. Annu Rev Mater Res. 1999; 29: 327–352. https://doi.org/10.1146/annurev.matsci.29.1.327
19. Heise S, Wirth T, Höhlinger M, Hernández YT, Ortiz J,Wagener V, Virtanen S, Boccaccini AR. Electrophoretic deposition of chitosan/bioactive glass/silica coatings on stainless steel and WE43 Mg alloy substrates. Surf Coat Technol. 2018; 344: 553–563. https://doi.org/10.1149/08201.0045ecst
20. Mahmoud ZS, Shams AK, Salman TA. Study the Inhibition Effect of Amoxicillin Drug for Corrosion of Carbon Steel in Saline Media. Baghdad Sci J. 2022; 19(1): 121-131. https://doi.org/10.21123/bsj.2022.19.1.0121
21. Maqubela LM. Corrosion Inhibition of Copper and Brass by Poly vinyl pyrrolidone – 2 – Acrylamide - 2-Methyl-Propansulphonate Composite in 1M Hydrochloric Acid. University of Johannesburg. master of technology. 2019. https://doi.org/10.20964/2019.01.46
22. Ahmed Z. Principles of Corrosion Engineering and Corrosion Control. 2016; 75: 40-52. 10.1016/B978-0-7506-5924-6.X5000-4
23. Salman TA, Samawi KA. and Shneine JK. Electrochemical and computational studies for mild steel Corrosion Inhibition by Benzaldehyde thiosemicarbazone in acidic medium Portugaliae Electrochimica Acta 2019; 37(4): 241-255. https://doi.org/10.4152/pea.201904241
24. Salman TA, Dhafer SZ, Shaimaa HJ, Moafaq AG, Ahmed M, Mohd ST, Ahmed AA. Effect of 1,3,4-thiadiazole scaffold on the corrosion inhibition of mild steel in acidic medium: an experimental and computational study. J Bio Tribo Corros. 2019; 48:1-11.https://doi.org/10.1007/s40735-019-0243-7
25. Ali TR., Salman TA. , Shihab MS. Pomelo leaves extract as a green corrosion inhibitor for carbon steel in 0.5 M HCl. Int J Scale Inhib. 2021; 10(4): 1729–1747. https://doi.org/10.17675/2305-6894-2021-10-4-23
26. SalmanTA, Qusay AJ, Mohammed AM, Ahmed AA, Lina MS, Kadhum AH, Mohd ST. New environmental friendly corrosion inhibitor of mild steel in hydrochloric acid solution: Adsorption and thermal studies. Cogent Eng. 2020; 7: 1826077. https://doi.org/10.1080/23311916.2020.1826077
27. Rana AH, Samawi KA, Salman TA. Inhibition Studies of Aluminium Alloy (2024) Corrosion in Acid Hydrochloride Solution Using an Expired Phenylphrine Drug Egypt J Chem. 2020; 63(8): 2863-2875. https://doi.org/10.21608/ejchem.2020.19583.2222
28. Hamadneh I, Alhayek H, Al-Mobydeen A, Abu Jaber A, Albuqain R, Alsotari S, Al-Dujaili A. Green Synthesis and Characterization of Yttrium Oxide, Copper Oxide and Barium Carbonate Nanoparticles Using Azadirachta Indica (the Neem Tree) Fruit Aqueous Extract. Egypt J Chem. 2019; 62 (4): 973-981. https://doi.org/10.21608/ejchem.2018.5281.1469
29. Rasha AJ, Muna SS, Farhan AM. Protection of Galvanized steel from corrosion in salt media using sulfur nanoparticles. Baghdad Sci J. 2022; 19(2): 347-354. https://doi.org/10.21123/bsj.2022.19.2.0347
30. Raheem HM., Salman TA. Tungsten Oxide Nanoparticles as Corrosion Inhibitor of Stainless Steel in Saline Medium. ANJS. 2020;.23 (1): 27 – 34. https://doi.org/10.22401/ANJS.23.1.04

Open Access **Baghdad Science Journal** **P-ISSN: 2078-8665**
Published Online First: April, 2023 **2023, 20(6): 2224-2233** **E-ISSN: 2411-7986**

فحص كفاءة تثبيط التآكل لجسيمات أوكسيد الإيتريوم النانوية المطلية على سبيكة الصلب الكربوني

مها جاسم حسين **تغريد علي سلمان**

قسم الكيمياء كلية العلوم، جامعة النهرين، بغداد، العراق

الخلاصة:

تظهر الجسيمات النانوية لأكسيد المعادن تفردًا في التطبيقات التقنية المختلفة نظرًا لخصائصها الفيزوكيميائية المناسبة. على وجه الخصوص ، فإن الجسيمات النانوية لأكسيد الإيتريوم (Y_2O_3NPs) مألوفة للتطبيقات التقنية بسبب ثابت العزل الكهربائي العالي وثباتها الحراري. يستخدم على نطاق واسع كمواد مضيفة لمجموعة متنوعة من المنشطات الأرضية النادرة ، والتصوير البيولوجي ، والعلاجات الضوئية. في هذه الدراسة تم اختيار جزيئات أوكسيد الإيتريوم النانوية (Y_2O_3NPs) كمثبط صديق للبيئة. تم التحقيق في التوصيف الفيزيائي والكيميائي لجزيئات أوكسيد الإيتريوم النانوية بواسطة مطيافية الاشعة تحت الحمراء (FT-IR) ، والتحليل الطيفي للأشعة فوق البنفسجية ، وانحراف الأشعة السينية (XRD) ، والفحص المجهري الإلكتروني (SEM) وطيف الأشعة السينية المشتتة للطاقة (EDX). يُظهر طيف FT-IR الذروة المميزة الرئيسية لـ YOY عند 565 cm^{-1} مما يشير إلى تكوين جزيئات أوكسيد الإيتريوم النانوية. كشف نمط XRD عن تشكيل هيكل مكعب أحادي الطور من YONPs. لوحظ التشكل السطحي بواسطة المجهر الالكتروني الماسح و أظهرت نتيجة طيف الاشعة السينية المشتتة أن تركيبة الإيتريوم والأكسجين في YONPs كانت 78.74% و 21.62% على التوالي. تم استخدام تقنية الترسيب الكهربائي لتراكيز مختلفة 0.15, 0.26 و0.3 عياري من جزيئات أوكسيد الإيتريوم النانوية كطلاء على سطح الفولاذ الكربوني وتم فحص السلوك المضاد للتآكل من خلال منحنى الاستقطاب في 18.204% محلول كلوريد الكالسيوم عند خمس درجات حراريه في المدى 293 – 313 كلفن. تشير النتائج التي تم الحصول عليها على ان جزيئات Y_2O_3NPs شكلت طبقة واقية تعمل كحاجز لحماية سبيكة الصلب الكربوني. بالإضافة الى ذلك, وجد أن طلاء بتركيز 0.26 عياري من جزيئات أوكسيد الإيتريوم النانوية أظهر كفاءة أفضل في الحماية من التآكل بالمقارنة مع طلاء بتراكيز 0.15 و 0.37 عياري ، على التوالي.

الكلمات المفتاحية: تشخيص مقاومة التآكل، الصلب الكربوني, ترسيب الترحيل الكهربائي ،الاستقطاب, الجسيمات النانوية لأكسيد الإيتريوم.